*Geophys. J. R. astr. Soc.* (1985) **83,** 75–92

# Shear-wave polarizations near the North Anatolian Fault – II. Interpretation in terms of crack-induced anisotropy

Stuart Crampin and David C. Booth *British Geological Survey, Murchison House, West Mains Road, Edinburgh EH9 3LA, Scotland*

Received 1984 August 30; in original form 1984 May 25

**Summary.** The polarizations of shear waves recorded by networks of digital three-component seismometers immediately above small earthquakes near the North Anatolian Fault in Turkey display shear-wave splitting on almost all shear-wave seismograms recorded within the shear-wave window. This splitting is incompatible with source radiation-patterns propagating through simple isotropic structures but is compatible with effective anisotropy of the internal structure of the rock along the ray paths. This paper interprets the phenomena in terms of widespread crack-induced anisotropy. Distributions of stress-induced cracks model many features of the observations, and synthetic polarization diagrams calculated for propagation through simulated cracked rock are similar to the observed patterns. This evidence for widespread crack-induced anisotropy lends strong support to the hypothesis of extensive-dilatancy anisotropy (EDA) suggested by laboratory experiments in subcritical crack-growth. The crucial evidence confirming some form of EDA would be observations of temporal changes in shear-wave splitting as the stress field alters the crack density and crack geometry. There is some weak evidence for such temporal changes at one site, but further analysis of suitable digital three-component seismometer networks in seismic areas is required to confirm EDA.

## 1 Introduction

Crampin, Evans & Üçer (1985) introduce two Turkish Dilatancy Projects: TDP1 in 1979 and TDP2 in 1980. These field experiments were designed to investigate the possibility of monitoring shear-wave splitting due to dilatancy-induced anisotropy by recording small earthquakes with closely-spaced networks of three-component instruments. All stress-induced cracks are necessarily aligned, and such aligned cracks will be effectively anisotropic to seismic wave propagation over a wide range of wavelengths and frequencies (Crampin 1978, 1984). Shear waves propagating through such cracked rock will split into two or more components with different velocities and different polarizations. Such effective anisotropy would cause the polarizations and delays between the split shear waves to vary with direction in systematic patterns characteristic of the anisotropy (Crampin 1981; Crampin & McGonigle 1981). Crampin,

Evans & Atkinson (1982, 1984) have proposed the hypothesis of extensive-dilatancy anisotropy (EDA) as a mechanism for this now commonly observed shear-wave splitting. The dilatancy is the result of subcritical crack growth (Atkinson 1979, 1984), possibly at low stress levels, extending existing cracks parallel to the direction of the maximum compressive stress.

The TDP recordings, digitized at 100 sample $s^{-1}$, are some of the first digital three-component traces of near earthquakes to be recorded within the shear-wave window on the surface immediately over the source, where the waveforms of shear waves can be directly interpreted in terms of the waveforms of the incident shear-waves (Booth & Crampin 1985; Evans 1984). These seismograms display features of shear-wave propagation at small epicentral distances not previously recorded. Phenomena which could be interpreted as anisotropy-induced shear-wave splitting have now been identified (Crampin *et al.* 1980; Booth *et al.* 1985) on many hundreds of shear wavetrains in these records. Two papers in this issue of *Geophys. J. R. astr. Soc.* report preliminary analysis of the TDP records: Evans *et al.* (1985) determine fault-plane mechanisms for the larger events; and Booth *et al.* (1985) analyse the shear-wave splitting and identify anisotropy along the ray path as the most likely cause of the phenomena. In addition, Doyle (1981) inverted earthquake arrival times from the TDP experiments for source location and anisotropy structure. This present paper interprets these observations in terms of widespread crack-induced anisotropy surrounding the fault zone, and calculated synthetic polarization patterns which model many characteristics of the observations.

## 2 Possible criteria for evaluating crack-induced anisotropy

Elastic anisotropy, or the effective elastic anisotropy of propagation through distributions of cracks with preferred orientations, has several effects on seismic waves. The two most important are that the velocity varies with direction, and that the wave motion is coupled in three dimensions so that characteristic signatures are written into the polarizations of the shear wavetrains.

### 2.1 VARIATION OF VELOCITY WITH DIRECTION

Probably the most widely recognized effect of anisotropy on the propagation of seismic waves is the variation of velocity with direction. However, the Earth has a complicated velocity structure, and the smooth variation with direction of velocities in any anisotropic layer within the Earth is difficult to identify with any reliability. Velocity variations due to anisotropy in the Earth can only be recognized in those rare occasions, such as *Pn* velocities in the oceanic mantle, when the velocities can be reliably measured for many directions in a single plane of a uniform anisotropic layer. In all other cases, particularly when the source position is not known, the velocity variation can only be estimated from a sophisticated inversion process, such as that of Doyle (1981), with many unknowns and many assumptions, and consequently with the possibility of many uncertainties and misinterpretations.

The dispersion of phase velocity with direction implies that the group velocity, the velocity of a packet of energy along a ray, deviates from the phase propagation direction so that the ray is not normal to the plane of constant phase. This deviation may be significant in numerical models, but because of the uncertainties associated with determining velocities in an inaccessible and poorly calibrated Earth structure, group velocity anomalies are unlikely to be easily identified in field observations. The deviation of group velocity from propagation direction is particularly difficult to recognise in observations of *P*-waves because the polarization of the particle displacement also deviates from the propagation direction in the same sense as the group-velocity deviation

(Crampin, Stephen & McGonigle 1982). These deviations may add considerable difficulties to the detailed interpretation of *P*-wave velocity anisotropy.

### 2.2 POLARIZATION ANOMALIES

A less widely recognized but equally fundamental feature of the behaviour of wave propagation in anisotropic solids is the three-dimensional coupling of the wave motion. Numerical experiments show that the effect of this coupling on shear waves, shear-wave splitting, is the most diagnostic phenomenon for recognizing and evaluating anisotropy by seismic wave propagation (Crampin 1978, 1981, 1985a). On entering a region of effective anisotropy, a shear wave necessarily splits into two or more components with the fixed polarizations and velocities appropriate for the particular direction of ray propagation. These split shear waves have different velocities and will separate in time, so that on re-entering an isotropic zone, or being recorded, the waveform of the original incident pulse cannot be reconstructed, and a characteristic signature is written into the shear wavetrain. This signature has remarkable properties: the single three-component shear wavetrain carries information about the three-dimensional structure of the crack geometry along the ray path.

Note that these split shear waves have different particle motion polarizations for different directions of propagation, and will only have *SV* and *SH* polarizations for propagation in specific symmetry directions through the anisotropy (Crampin 1978).

There are four phenomena which may be used to identify the effects of crack-induced anisotropy on the polarizations of shear wavetrains:

(1) shear waves should display shear-wave splitting in most directions of propagation (although there are some restrictions on recordings made at the free surface, see the next paragraph);

(2) the variation with direction of the polarization of the split shear waves should show characteristic patterns dependent on the effective anisotropic symmetry of the particular crack geometry – these can be conveniently displayed in equal-area projections of a hemisphere of directions (Crampin & McGonigle 1981); and

(3) the variation with direction of the delays between the split shear-waves should also show characteristic patterns dependent on the crack geometry (Crampin & McGonigle 1981). Furthermore, if the stress controlling the crack distribution changes, the pattern of polarizations and delays would also be expected to vary with time, so that:

(4) the patterns of polarizations and delays may show temporal variations if the changes in stress result in significant modifications to the crack density and geometry.

Numerical experiments (Crampin 1978, 1981, 1985a) show that shear-wave splitting within the interior of a solid may be most easily recognized by plotting the particle motion in polarization diagrams for a series of time windows along the three-component seismograms. Such experiments show that the polarization of the faster split shear wave is a stable phenomenon. The polarization depends on the symmetry of the anisotropy along that particular direction of propagation, and equal-area projections of the variations displayed by the polarizations may be used to identify the orientations of the crack geometry. However, shear waves have complicated interactions at free surfaces and there are constraints on interpreting shear waves at the free surface (Evans 1984; Booth & Crampin 1985). For angles of incidence greater than a critical angle $\sin^{-1}(V_S/V_P) \cong 35°$ (the exact value depends on Poisson's ratio and on the curvature of the wavefront), shear waves observed at the surface are subject to phase and amplitude changes, and mode conversions which seriously modify the incident waveforms and polarizations. (Shear waves observed below the surface in VSPs are free of these surface interactions, although there may be interference from surface reflections.) Booth & Crampin (1985) demonstrate these effects with synthetic shear waves incident on an isotropic free surface. Only for incidence angles

less than critical, can the splitting of the incident shear wave be easily interpreted from observations at the free surface. This zone within the critical angle of incidence is called the *shear-wave window*. This limitation to incidence within the shear-wave window places severe constraints on the deployment of seismometers over earthquakes, since the useful aperture for shear-wave analysis of a network centred over the source region is small (approximately twice the focal depth). Even within the shear-wave window there may be disturbing phases focused by irregular topography and from reverberations in low-velocity surface layers. It is fortunate for the interpretation of the TDP records, that irregular topography appears to scatter rather than focus disturbing arrivals (Booth *et al.* 1985), and that hard rock outcrops occur throughout the aperture of the network so that near-surface reverberations are limited.

### 2.3 VARIATION OF ATTENUATION WITH DIRECTION

The attenuation of seismic waves propagating through cracks with preferred directions of alignment may also show marked variations with the direction of propagation. Hudson (1981, 1982) also derives theoretical formulations for the attenuation of seismic body waves through cracked rock (see Crampin 1984). This attenuation can be represented as the imaginary part of complex anisotropic elastic constants allowing synthetic seismograms to be calculated modelling both velocity and attenuation variations with direction (Crampin 1981).

Shear-wave splitting again shows the most distinctive variations of attenuation, and in order to evaluate the effects of anisotropic attenuation three-component recording is necessary. Attenuation is difficult to evaluate, however, without detailed knowledge of the source signal. Since the analysis of crack-induced attenuation requires identification of shear-wave splitting, it is expected that the signature of polarization anomalies written into the shear wavetrains will be more valuable for diagnosing and evaluating crack-induced anisotropy than variations of attenuation.

Note also that, in general, attenuation due to cracks is inversely related to the velocity variation, so that the largest attenuation of any body wave occurs in those directions in which the velocity is least (Crampin 1984). This behaviour reinforces observations of the faster first arrival of the split shear waves, since slower later arrivals suffer relatively greater attenuation and are superimposed on the coda of the first arrivals.

## 3 Possible crack geometries near the North Anatolian Fault

There are four main ways in which information about the possible density and geometry of a crack distribution can be estimated from seismic observations at the surface. These are:

(1) Fault-plane solutions, where the positions of the nodal planes place some constraints on the possible orientations of the stress fields common to both focal mechanisms and dilatancy cracking.

(2) Polarizations of the shear waves, within the shear-wave window, where the orientation of the shear waves is controlled by the three-dimensional symmetry of the crack geometry along the particular ray paths.

(3) Delays between shear waves within the shear-wave window, where both polarizations and delays in synthetic seismograms vary with direction in characteristic patterns fixed by the orientation and geometry of the crack distribution. Note, however, that the arrival of slower secondary shear waves is superimposed on the coda of the first split shear wave, so that the polarizations of later arrivals and their arrival times, which determine the delays, are difficult to estimate with any reliability.

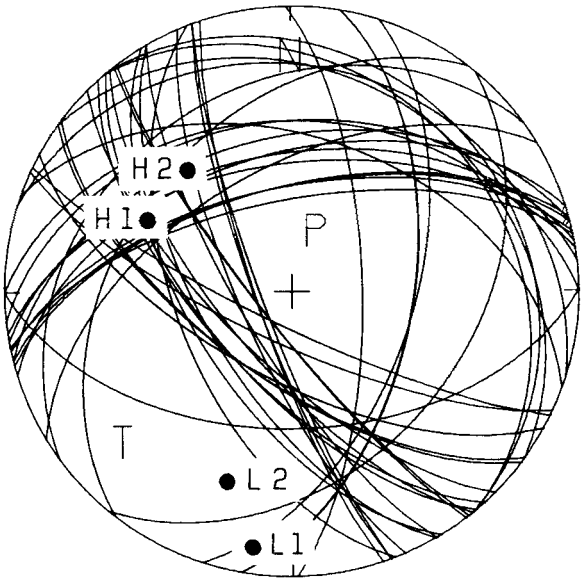


**Figure 1.** Nodal lines of the TDP2 fault-plane mechanisms from fig. 3 of Evans *et al.* (1985) superimposed in an equal-area plot of the upper focal sphere. The segments of the tensional (T) and compressional (P) quadrants common to all solution are marked. The axes of high *P*-wave velocity and low *P*-wave velocity of the arrival-time inversions of Doyle (1981) are marked by H1 and L1 for TDP1, and H2 and L2 for TDP2, respectively.

(4) The anisotropic structure derived from inversions of arrival-time data should also be compatible with the crack-induced anisotropy.

### 3.1 FAULT-PLANE MECHANISMS

Evans *et al.* (1985) determine fault-plane solutions for 23 of the larger TDP2 earthquakes. They find a wide range of mechanisms, and, although the individual mechanisms have too few polarity points to be well constrained, the horizontal projections of the slip vectors of the microearthquakes are consistent with the general trend of slip vectors from mechanisms of major earthquakes around the North Anatolian Fault (NAF). The most probable interpretation of this is that the small earthquakes of the TDP swarm are driven by the overall tectonic stress in the region acting on individual facets of a complicated fault zone.

Fig. 1 shows the nodal lines of these 23 solutions (from fig. 3 of Evans *et al.* 1985) overlain in one equal-area plot of the upper focal sphere. There are a range of mechanisms, but the marked segments of the focal sphere show areas of the tensional (T) and compressional (P) quadrants which are common to all solutions. There is generally normal faulting on a system of fault planes, or facets of fault planes, subject to an overall stress field with the principal axes of stress within the common segments marked in Fig. 1. The near-vertical compressive axis is unlikely to be the dominant stress controlling the micro-earthquakes, and we conclude that a near-horizontal principal axis of tension is the main driving force on this small section of the NAF. The north side of this section is the boundary of the Black Sea region of the massive Russian plate, and the south side is the narrow end of the wedge-shaped Marmara micro-plate which is rotated and sheared as the wider end is forced against the bulge of Thrace on the margin of the Black Sea plate at the western end of the Marmara Sea (Evans *et al.* 1985). Thus a major tensional driving force is consistent with the tectonics at this narrow end of the wedge-shaped Marmara block. It should be

noted that swarm events in California are also associated with extensional regimes (Weaver & Hill 1978).

The focal mechanism of earthquakes is of critical importance for studies of shear-wave polarizations for two reasons. The focal mechanisms determines the polarity and polarization of the shear-waves radiated from the source. Secondly, the orientations of the focal mechanisms and the dilatancy cracks are both determined (although not necessarily directly) by the same system of stresses.

Tri-axial systems of stress with $\sigma_1 \geqq \sigma_2 \gg \sigma_3$ (compression positive) are likely to result in parallel cracks perpendicular to the $\sigma_3$-direction (see the interpretation by Crampin *et al.* 1984 of a laboratory experiment by Hadley 1975). If the $\sigma_3$-direction is horizontal, the orientation of such cracks would tend to be vertical, and normal to the horizontal tension driving the TDP micro-earthquakes. Thus the strike of the cracks should be between east–west and north-west–south-east perpendicular to the range of possible principal directions of tension in the common tensional segment in Fig. 1.

The theoretical polarizations of shear waves radiating from the 23 TDP mechanisms determined by Evans *et al.* (1985) show a preferred alignment of N 50°E for arrivals within the shear-wave window (see fig. 4a of Booth *et al.* 1985), that is very close to the mean of the horizontal projections of the slip vector in the tensional quadrant of the fault plane mechanism. It is an important discriminant that the polarizations of the shear waves from a fault-plane mechanism tend to be in the *tensional* quadrant, whereas the strike of dilatancy cracks (and, as we shall see in the next section, the polarizations of the faster split shear waves propagating through dilatancy cracks) will tend to align parallel to the principal axis in the *compressional* quadrant. The observed polarizations in fig. 2 of Booth *et al.* (1985) lie within the compressional quadrant. Thus, they are incompatible with the polarizations radiated directly from the source, but are compatible with the effects of aligned cracks along the ray paths.

### 3.2 THE VARIATIONS OF SHEAR-WAVE POLARIZATIONS

Fig. 1 of Booth *et al.* (1985) show that the mean of the polarizations within the shear-wave window of the faster split shear waves observed during the TDP experiments are (with the exception of those at one recording site) within ±20° of N 100°E for all arrivals at all recording sites. Crampin & McGonigle (1981) model theoretical polarizations for various anisotropic solids simulating crack distributions. In distributions of both dry and saturated vertical parallel cracks, the polarizations of the faster split shear wave recorded by horizontal instruments are parallel to the strike of the cracks throughout most of the shear-wave window. Note that Crampin & McGonigle use stereographic projections rather than equal-area plots, and model cracks with less satisfactory theoretical formulations than those now preferred (see Fig. 2), but that these differences produce only minor differences in the patterns of variations. Crampin & McGonigle also use projections of the *upper hemisphere* of directions, whereas we now use projections of the *lower hemisphere* simulating the behaviour of arrivals at the azimuths as recorded by instruments on the surface.

Also note that in the analysis of the TDP1 and TDP2 experiments we have used polarization directions without discussing the polarity of the direction (with the exception of fig. 5 of Booth *et al.* 1985). We have been forced to do this because, as we have seen, the polarity of the polarization is dependent on the radiation from the source, and in the TDP1 and TDP2 experiments we can only estimate the source polarities and orientations from the very small number of focal mechanisms that were determined by Evans *et al.* (1985) for TDP2. The orientations of the (undirected) polarizations of the first shear-wave arrival observed are fixed by the direction of the propagation path through the anisotropy, so that we can use the undirected polarizations to estimate the anisotropic symmetry along the ray path. The polarization of the radiation from the

source determines the division of energy between the shear waves split by the anisotropy, and may have a major effect on the polarization diagrams traced by three-component wave displacements, but does not affect the orientation of the initial onset of the faster split shear wave.

### 3.3 SHEAR-WAVE DELAYS

Numerical experiments show that polarizations are changed very little by variations in crack density and variations in the rock matrix if the overall symmetry of the crack geometry is retained (Crampin 1978). In contrast, the delays between split shear waves are very sensitive to variations and discontinuities along the ray path (some of the reasons are discussed in the Appendix). Consequently, it is not unexpected that the delays between the split shear waves observed during the TDP experiments show no recognizable patterns when displayed in equal-area projections (Booth *et al.* 1985). However, the maximum delay observed at any station during TDP1 and TDP2 is the equivalent of a delay of 0.14 s over a distance of 10 km, and we have used this maximum value as a guide to possible crack densities.

### 3.4 MODEL CRACK DISTRIBUTIONS

The simplest crack geometry satisfying the parallel alignments of the polarizations of the first shear-wave arrivals (Booth *et al.* 1985) and the observations discussed in the previous three sections is a distribution of parallel vertical cracks. Transverse isotropy between the source and the receiver, whether caused by aligned cracks or fine layering, is ruled out because the observed first shear-wave polarizations are approximately *parallel* and clearly different from the *radial* distribution of polarization alignments on the surface of a transversely isotropic medium

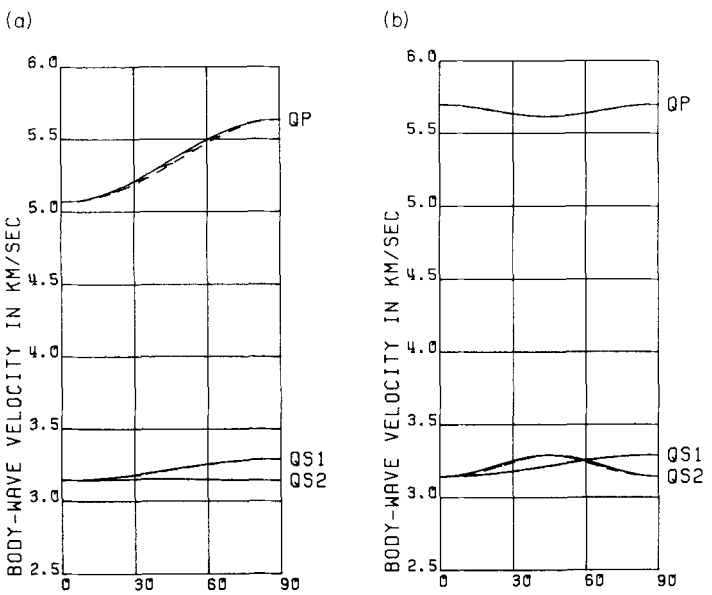


**Figure 2.** The variation with direction of body-wave velocities in distributions of (a) dry and (b) liquid-filled parallel cracks in an isotropic solid ($\varrho$=2.6 g cm$^{-3}$, $V_P$=5.7 km s$^{-1}$, $V_S$=3.29 km s$^{-1}$) with crack densities $Na^3/v$=0.04, where $N$ is the number of cracks of radius $a$ in volume $v$. The angle of incidence to the crack face of phase propagation direction (solid lines) varies from 0° to 90°, phase velocities are solid lines, and group velocities are broken lines. Corresponding values of phase and group velocity are joined every 10° of phase velocity direction. The modelling follows the formulations of Hudson (1981, 1982) as adopted by Crampin (1984).

(Crampin & McGonigle 1981). Fig. 2 shows the velocity variations in distributions of dry and fluid-filled parallel cracks with crack densities of 0.04 modelling the maximum observed delay between the split shear waves. The rock matrix (assumed to be isotropic) is the half-space of the simple isotropic structure determined by Crampin *et al.* (1985) from analysis of quarry blasts ($V_P$=5.7, $V_S$=3.3 km s$^{-1}$). The variation with direction of the effects of homogeneous crack distributions on shear-wave propagation can be illustrated by projections of the horizontal polarizations, and projections of the (normalized) delays. Equal-area lower-hemisphere projections of the polarizations and delays are shown in Fig. 3 for the distributions of the dry and liquid-filled cracks in Fig. 2 for vertical cracks and for cracks dipping 15° and 30° to the south (measured from the vertical). The strike of the cracks is N 100°E. The vertical cracks and those dipping at 15° show parallel polarizations over the whole or nearly the whole shear-wave window. We cannot expect that the theoretical formulations for uniform distributions of smooth penny-shaped cracks will closely model cracks in the real Earth. However, as a first approximation, the observed orientations of the shear-wave polarizations in the TDP experiments can be modelled by propagation through dry or liquid-filled approximately vertical cracks with a strike of about N 100°E. Such vertical alignments of cracks are expected in regions with a non-lithostatic stress field as is shown by the vertical cracks produced by most hydraulic fracturing operations (Hubbert & Willis 1957; Zoback & Zoback 1980).

Delays between split shear waves are likely to be distorted, for the reasons given in the Appendix, and the observed delays do not show any recognizable pattern, although the maximum delay in Fig. 3 is modelled on the maximum observed delay.

### 3.5 ARRIVAL-TIME INVERSIONS

The arrival-time inversions of Doyle (1981) are strongly dependent on *P*-wave arrivals, and shear-wave arrival times and shear-wave delays have much less influence on the solution. Thus, when interpreting solutions in terms of crack distributions, axes of low *P*-wave velocity would be associated with the direction of tensional stress normal to the planes of the major crack distributions. Similarly, axes of high *P*-wave velocity would be associated with directions of compressive stress parallel to the planes of the major crack distributions.

Doyle (1981) lists the principal axes of the preferred solutions of inversions for TDP1and TDP2. The high- and low-velocity axes are marked in Fig. 1 on the plot of the common compressional and tensional segments of the fault-plane solutions of Evans *et al.* (1985). The low-velocity (tensional) axes are in, and within 10° of the common tensional segment for TDP2 and TDP1, respectively, and the high-velocity (compressional) axes are within 20° of the common compressional segment for both TDP1 and TDP2. Since the fault-plane solutions and the arrival-time inversions are derived from completely independent measurements and subject to different sources of error, the near agreement of the axes is better than might have been expected and lends support to the overall concept of widespread crack-induced anisotropy.

Note that the equal-area plots in Fig. 1 are of the *upper-hemisphere* above the earthquake foci, whereas the equal-area plots in Fig. 3 are of the *lower-hemisphere* beneath the recording sites. A rotation of 180° is required to bring the directions into equivalence.

## 4 Polarization diagrams

Polarization diagrams of the particle displacements of *plane* shear-waves display distinctive patterns of motion diagnostic of the presence of anisotropy, which may be used to estimate some of the properties of the anisotropic media through which the waves are propagating (Crampin 1978, 1985a). Plane-wave approximations are not appropriate for modelling the behaviour of

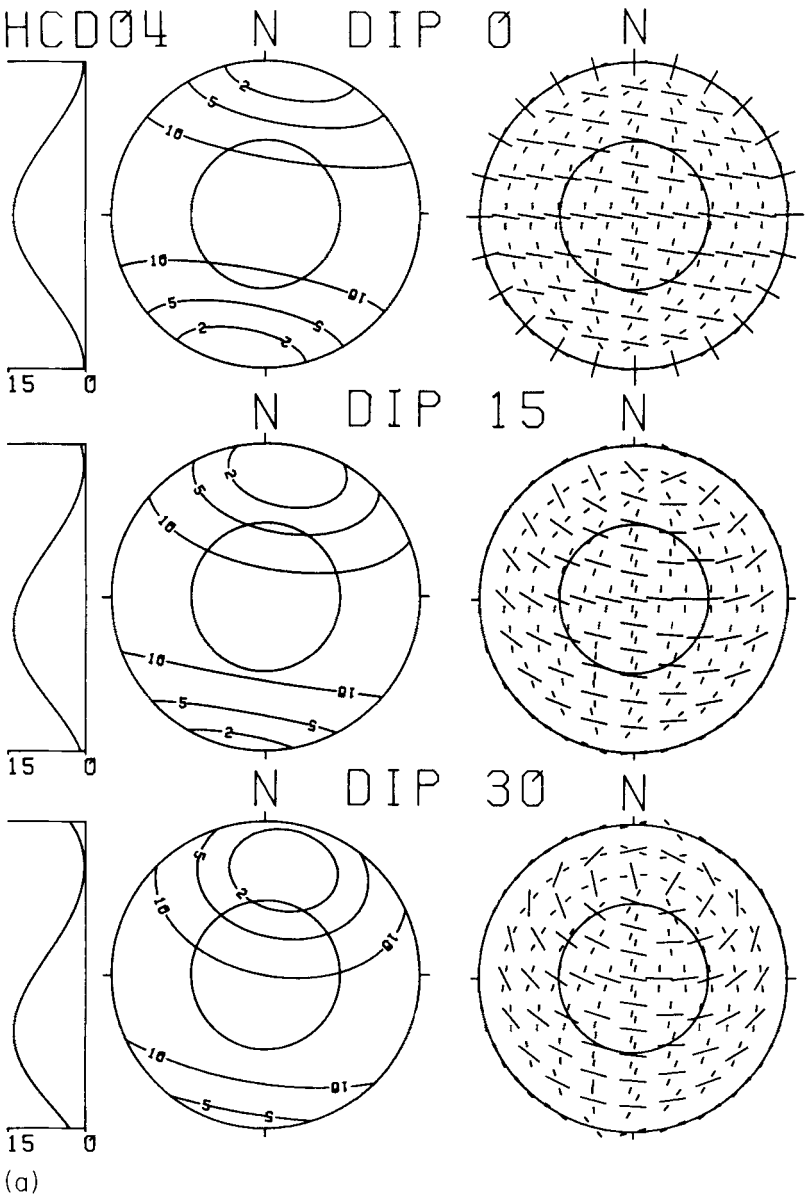


**Figure 3.** Equal-area projections of the lower hemisphere of the delays (to the left) and the horizontal polarizations (to the right) of shear-waves split by propagation through the (a) dry and (b) liquid-filled parallel crack distributions of Fig. 2. The cracks strike N 100°E so that the polarizations model the observations. The upper sets of figures are projections for parallel vertical cracks, and the middle, and lower sets are for parallel cracks with crack normals dipping 15°, and 30° northwards, respectively. The contoured delays are labelled in hundredths of a second simulating propagation through a hemisphere of 10 km radius. North–south sections of the contoured delays are shown to the left of the contoured delays. The solid lines in the projections of the polarizations are the faster, and the broken lines, the slower split shear wave. A circle has been drawn at an incidence angle at 40° to indicate the approximate shear-wave window from a point source.

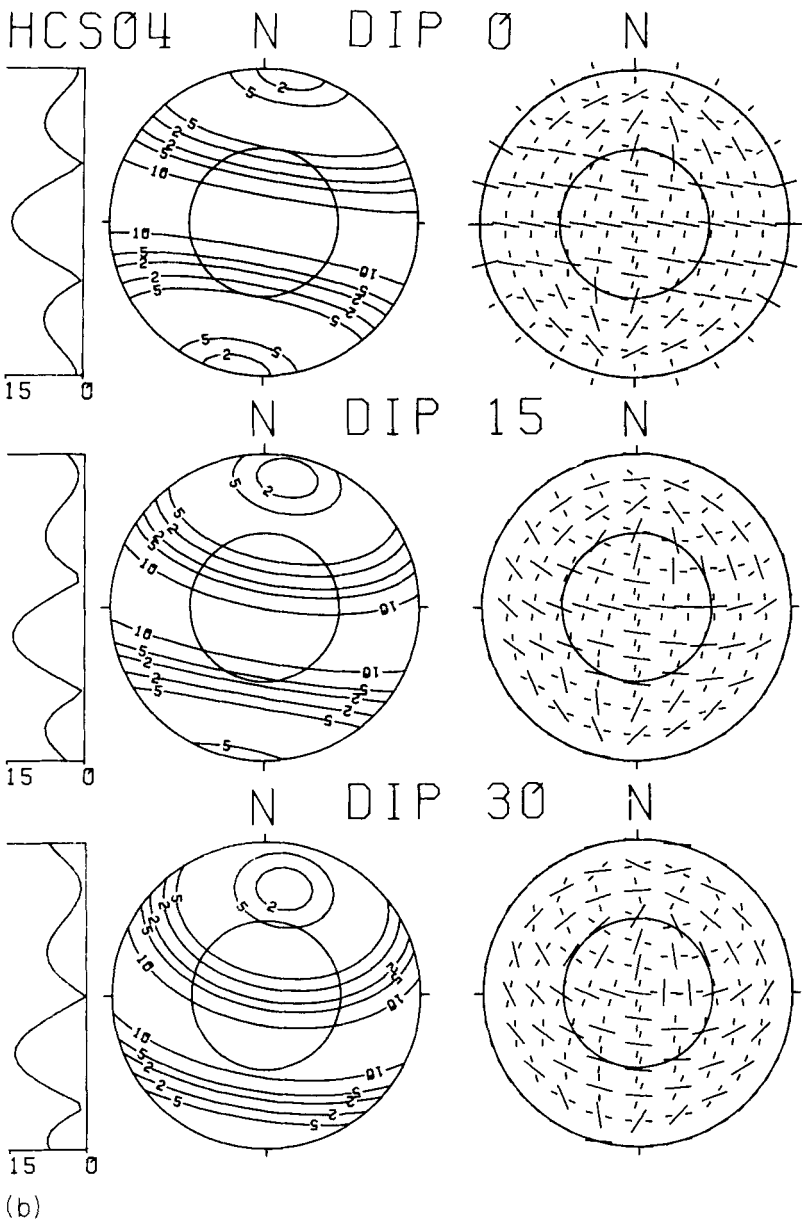


**Figure 3** – *continued*

shear waves in the TDP experiments because the curvature of the wavefronts at the surface, and the interactions of the shear waves with the free surface, seriously distort the incident waveforms (Booth & Crampin 1985). Consequently, we use the cylindrical approximation of the anisotropic reflectivity technique (Booth & Crampin 1983) to evaluate synthetic seismograms on a curved wavefront and to model the polarization diagrams from the TDP experiments.

The characteristic patterns in polarization diagrams show wide variations with any combination of elliptical, linear, and cruciform motion being possible (Crampin 1978, 1985a). The patterns are very sensitive to the properties of the waveforms and the structures. The exact pattern being dependent on: the polarization, the polarity, the frequency or wavelength, the waveform, and the

number of cycles of the incident wave; the direction and length of the path through the cracked rock; the crack density and orientation of the crack geometry along that path; and the orientation of the plane sections in the polarization diagrams. It might be thought, that with such wide variations possible, polarization diagrams would be impossible to interpret. However, despite the great variety in the patterns of polarization, the orientation of the polarization of the faster split shear wave appears to be a remarkably stable feature for the particular direction of propagation through effectively anisotropic rock (Crampin 1985a). The pattern of (undirected) polarizations, displayed in stereographic or equal-area projections, is characteristic of the symmetry of the crack geometry along the path.

Fig. 4 compares synthetic polarization patterns with observed patterns in the TDP records. The synthetic polarization diagrams are calculated for shear waves arriving from a range of azimuths

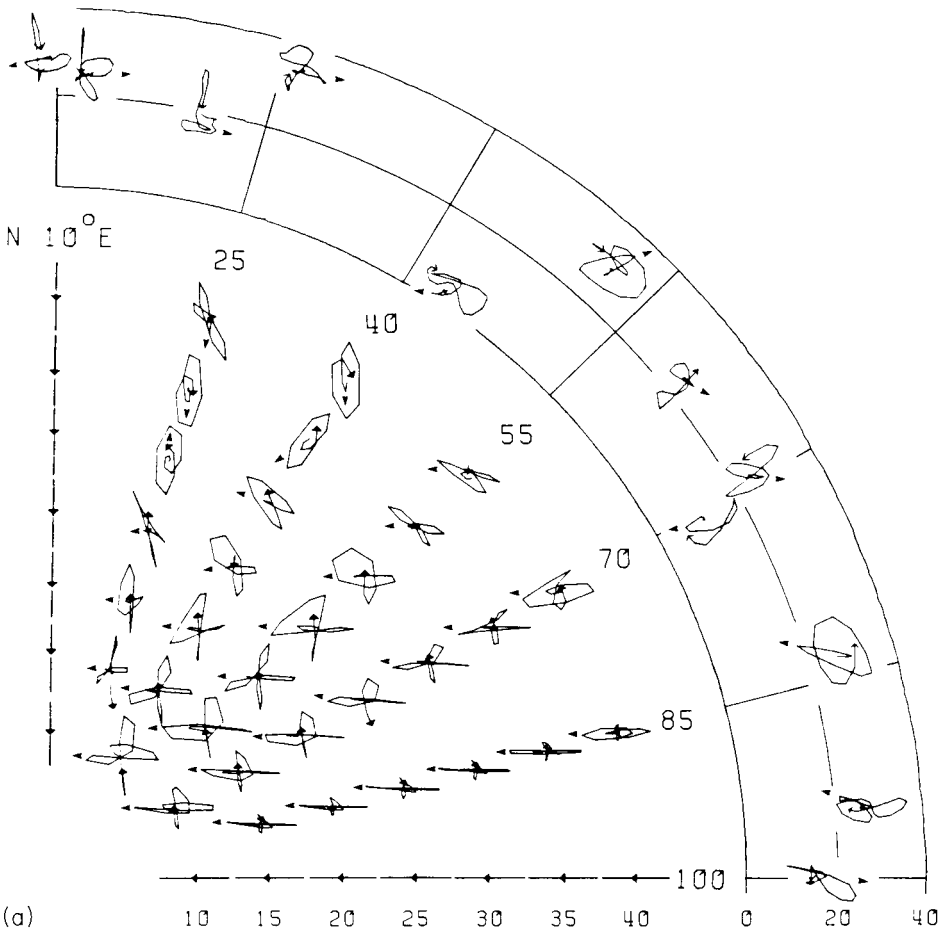


**Figure 4.** Polarization diagrams of 10 Hz synthetic shear-wave seismograms, plotted within the marked azimuth angles, are from a point source at 10 km depth for receivers on the surface of an homogeneous half-space modelling the liquid-filled cracks of Figs 2(b) and 3(b). The cracks are oriented vertically with a strike of N 100°E. The diagrams are calculated for a range of incident angles from 10° in steps of 5° to 40° and a range of azimuths from N 10°E in steps of 15° to N 100°E. The incident shear waves are polarized: (a) *SV*; (b) *SV*45*SH* (a shear wave with polarization bisecting *SV* and *SH*) – the bottom line of polarization diagrams are calculated at the same incidence angles through an equivalent *isotropic* half-space; and (c) *SH*. Outside the azimuths angles are observed polarization patterns recorded within the shear-wave window from 10 TDP1 earthquakes. They are located in the quadrant which best models the observations and positioned along the correct azimuth and the approximate incidence angle.

in the NE quadrant, and a range of incidence angles within the shear-wave window above a point source at 10 km depth in a half-space of the vertical liquid-filled cracks of Fig. 2. The superficial thin layer in the structure used for event location (Crampin *et al.* 1985) was not used in modelling polarizations, after tests had shown that its inclusion did not result in significant changes in the synthetic polarizations, although there were substantial increases in computing costs. The strike of the cracks is N 100°E modelling the polarizations of the incident shear waves (Booth *et al.* 1985). Polarization diagrams are drawn for three polarizations of the initial shear waves radiated from the source in Fig. 4(a, b, c).

These polarizations of the initial shear waves are the only difference between the models for the three quadrants. The synthetic diagrams vary widely for different azimuths and incident angles within each quadrant and there are wide differences in diagrams between the quadrants. However, despite the great variety of diagrams the polarizations of the initial shear-wave displacements (marked by arrow heads) *are approximately parallel to the strike of the vertical cracks* except for a few particular combinations. These exceptional combinations occur when:

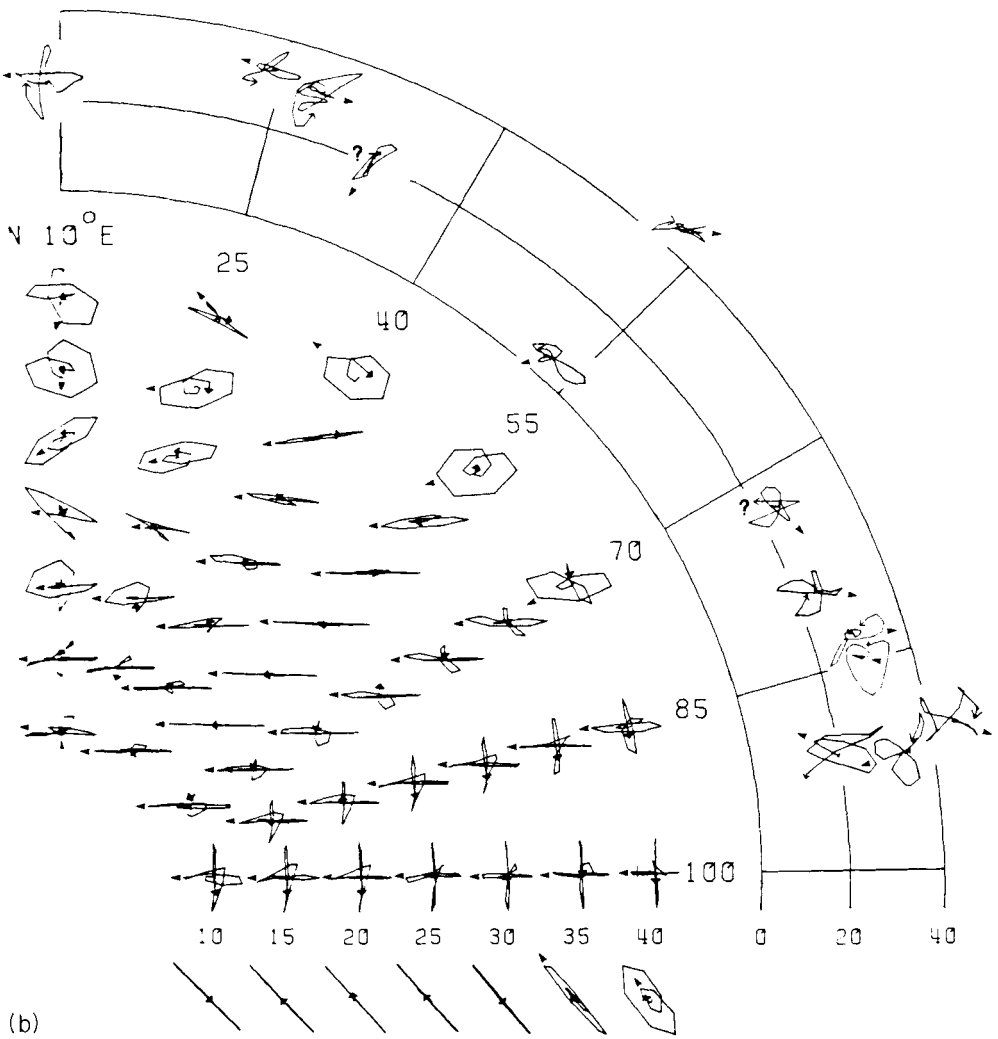


**Figure 4** – *continued*

(1) there is no initial displacement parallel to the polarization of the faster shear wave, so that only the slower shear wave is excited – this occurs for all angles of incidence at azimuth N 10°E in Fig. 4(a) and at azimuth N 100°E in Fig. 4(c);

(2) the faster split shear waves become approximately normal to the strike of the cracks in all quadrants for incidence greater than about 30° at azimuths from N 10° to N 45° (this is because the shear-wave sheets intersect within the shear-wave window along these azimuths, see Figs 2b and 3b), also near these intersections the delays are small and there are elliptical polarization diagrams;

(3) the angle of incidence is near the edge of the shear-wave window and the polarization patterns at the surface may be severely modified by the interaction with the free surface – this is common near incidence of 40° at all azimuths in all three quadrants.

The 37 observed shear-wave polarization diagrams in Fig. 4 are from 10 earthquakes chosen at random throughout the TDP1 sequence from those earthquakes which had three or four arrivals within the shear-wave window, but excluding arrivals from the anomalous site PA. The observations are positioned at the correct azimuths and incidence angles and plotted on the quadrant which appears to have the most appropriate patterns at neighbouring azimuths, having made allowance that the quadrants are calculated only for three possible shear-wave

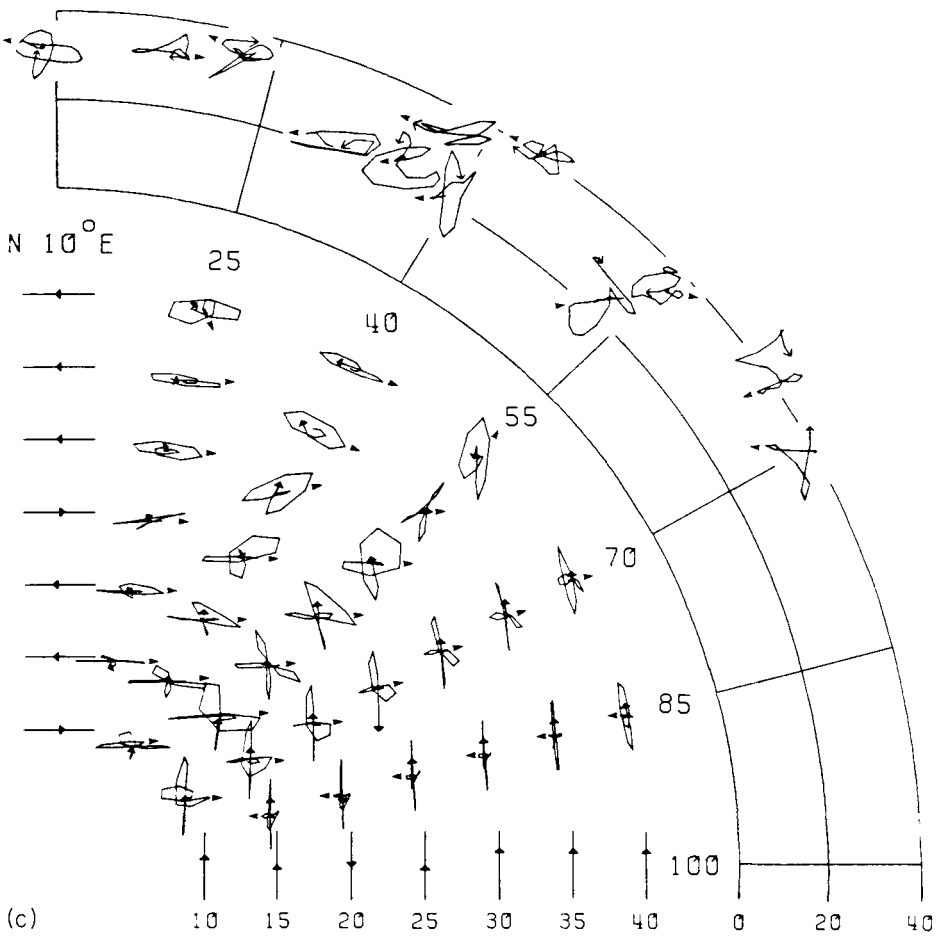


**Figure 4** – *continued*

polarizations at the source. As noted in the Appendix, the incidence angles of the observations may have comparatively large errors, and as is to be expected from the many factors influencing the diagrams, the observed diagrams seldom match the synthetic diagrams exactly. However, we suggest that the observed and synthetic polarization diagrams have two remarkable similarities:

(1) Almost all polarization diagrams show clear signs of splitting, where the nearly linear polarization of the first shear arrival is abruptly changed by the arrival of a second shear wave with a different polarization. Such phenomena are inexplicible in terms of the behaviour of the radiation from a small double-couple source and propagation through an isotropic structure. Examples of the near-linear polarizations in equivalent isotropic models are given below the quadrant in Fig. 4(b).

(2) The initial polarization of almost all the first arrival shear waves is parallel to the strike of the simulated cracks in the model for the calculations. The only exceptions to the parallel onsets in the synthetic patterns are the specific directions mentioned in the previous paragraph. The only major exceptions to the parallel onsets among the observations are in Fig. 4(b) at azimuths N 32°E and N 73°E. Even here there are small precursory polarizations, marked by question marks, that are parallel to the overall parallel trend and this small arrival may be the faster shear wave which has not been correctly identified because the second arrival has the dominant amplitude.

## 5 Conclusions

Booth *et al.* (1985) show that the polarizations of the faster split shear waves, observed within the shear-wave window at the surface during the TDP experiments, are approximately parallel. This is not consistent with the expected orientations of shear waves radiated from the estimated source mechanisms through an isotropic crust. Booth *et al.* suggest that the polarizations are controlled by the effective anisotropy along the ray paths. This paper shows that anisotropic structures simulating parallel nearly-vertical cracks can model many of the observed features, including many of the characteristics of the observed polarization diagrams.

There are six, largely independent, phenomena supporting some form of (crack-induced) anisotropy:

(1) Almost all shear waves arriving within the shear-wave window display the split arrivals indicative of propagation through the effective elastic anisotropy resulting from stress-induced cracking.

(2) The polarizations of the faster split shear waves are nearly parallel at all recording sites (with one exception), and such parallel alignments are characteristic of shear-wave propagation through distributions of parallel vertical cracks. It should be noted that parallel alignments are almost the only pattern that can easily be identified with a crack distribution. Thus it is a fortunate coincidence that the common stress distribution in the Earth, horizontal directions of maximum tension or minimum compression, results in parallel vertical cracks with an effective anisotropy with easily identifiable patterns of polarization.

(3) Many essential characteristics of the observed polarization diagrams are similar to the characteristics in diagrams of synthetic seismograms calculated from sources at appropriate depths and distances in an effectively anisotropic half-space modelling the structure surrounding the TDP earthquake activity.

(4) The orientation of the effective crack-induced anisotropy derived from the shear-wave polarizations is consistent with the common directions of compression and tension in fault-plane mechanisms of the TDP earthquakes.

(5) The orientation of the principal axes of the anisotropy derived from inversions of the TDP

arrival times is reasonably consistent with the common directions of compression and tension in the fault-plane mechanisms.

(6) There are some indications that the effective anisotropy at one site may have varied with time as would be expected if the stress changes enough to alter the crack geometry.

These phenomena have been modelled by the effective anisotropy of liquid-filled cracks having relative *P*-wave velocity-anisotropy of 2 per cent. Such comparatively small *P*-wave anisotropy would be very unlikely to be detected in conventional analysis based on arrival-time analysis in isotropic structures. The shear-wave velocity-anisotropy is also small, about 4.5 per cent, but is large enough to show the fundamental differences in the behaviour of (synthetic) shear-wave polarizations in Fig. 4. We suggest that the overall consistency of this range of different seismic phenomena lends strong support to the existence of distributions of stress-induced cracks pervading the North Anatolian Fault zone.

Since these observations suggest that anisotropy is uniformly present in much of the rock surrounding the fault zone, such cracks cannot be caused by dilatancy at high stress concentrations, but must be a comparatively low-stress, low-strain phenomenon. Extensive-dilatancy anisotropy has been suggested by Crampin *et al.* (1984), where the dilatancy is likely to be the result of subcritical crack growth in preferred directions perpendicular to the direction of least compressive stress.

As has been stated elsewhere (Crampin 1978; Crampin *et al.* 1984), the crucial observation, which would confirm the hypothesis that the observed shear-wave splitting is caused by crack-induced anisotropy, would be the correlation of temporal changes in the behaviour of the splitting with stress changes during an earthquake episode. The apparent change in the polarization between station PA in 1979 and station PB in 1980, 1.2 km distant, could be associated with stress released by a small local earthquake recorded by the Kandilli network in the interval between TDP1 and TDP2 (Booth *et al.* 1985). Unfortunately we know too few details about the local structure or the local earthquake activity in the intervening period for this to be more than a promising indication. However, the North Anatolian Fault has been subject to a more or less consistent stress field for 6 Myr. It cannot be expected that the comparatively small magnitude earthquakes of the TDP swarm are significantly going to alter the local stress distribution imposed by the regional stress pattern except in exceptional circumstances. Such circumstances might occur if there is an accumulation of stress very local to a particular site (since the polarization of the initial shear-wave onset is primarily determined by the structure near the recording site), or in the build-up of regional stress before a major earthquake. Note that the region of the TDP swarm has been designated a seismic gap by Toksöz, Shakal & Michael (1979). Thus it is of interest to continue to monitor the shear-wave polarizations in the TDP networks in the future and a further experiment, TDP3, recorded the swarm events in a variety of configurations for six months in 1984.

Thus, convincing evidence for temporal variations in shear-wave splitting as a result of stress changes must await further observations. If such extensive-dilatancy anisotropy could be confirmed, it would suggest that the build-up of stress before a large earthquake could be monitored by shear-wave splitting in the shear wavetrains of local earthquakes, or, ideally, in reflection lines with a shear-vibrator source. This could have major implications for earthquake prediction research, as well as major implications for the behaviour of many tectonic processes in the crust.

Recent publications in the USSR (Gal'perin 1977) and unpublished reports from the oil industry in the West indicate that shear-wave splitting is almost routinely observed whenever three-component vertical seismic profiles record shear-wave vibrators. Observed patterns of polarization are similar to the synthetic polarization patterns calculated for shear wave

propagation through a layer of aligned cracks in Crampin (1985a). This suggests that extensive-dilatancy anisotropy may exist throughout much of the upper brittle section of the crust, where the cracks are aligned with respect to the prevailing plate motion (Crampin 1985b; Crampin & Atkinson 1985). This shear-wave anisotropy was not noticed previously because most seismic investigations have analysed *P*-waves recorded principally on single-component vertical instruments, and liquid-filled cracks have little effect on *P*-wave propagation. Recent advances in instrumentation and digital three-component recording now result in shear-wave splitting being frequently observed in digital three-component records. Numerical models show that the isotropic *P*-wave velocity model of the crust, which has been so extraordinarily successful in so many applications, can co-exist with the anisotropic shear-wave model with little conflict or disagreement.

## Acknowledgments

The work was supported by the Natural Environment Research Council and is published with the approval of the Director of the British Geological Survey. Some indirect support was provided by USGS Contract No. 110196.

## References

Atkinson, B. K., 1979. A fracture mechanics study of subcritical tensile cracking of quartz in wet environments, *Pure appl. Geophys.*, **117,** 1011–1124.

Atkinson, B. K., 1984. Subcritical crack growth in geological materials, *J. geophys. Res.*, **89,** 4077–4114.

Booth, D. C. & Crampin, S., 1983. The anisotropic reflectivity technique: theory, *Geophys. J. R. astr. Soc.*, **72,** 755–766.

Booth, D. C. & Crampin, S., 1985. Shear-wave polarizations on a curved wavefront at an isotropic free surface, *Geophys. J. R. astr. Soc.*, **83,** 31–45.

Booth, D. C., Crampin, S., Evans, R. & Roberts, G., 1985. Shear-wave polarizations near the North Anatolian Fault – I. Evidence for anisotropy-induced shear-wave splitting, *Geophys. J. R. astr. Soc.*, **83,** 61–73.

Cormier, V. F., 1984. The polarization of *S* waves in a heterogeneous isotropic Earth model, *J. Geophys.*, **56,** 20–23.

Crampin, S., 1978. Seismic wave propagation through a cracked solid: polarization as a possible dilatancy diagnostic, *Geophys. J. R. astr. Soc.*, **53,** 467–496.

Crampin, S., 1981. A review of wave motion in anisotropic and cracked elastic-media, *Wave Motion*, **3,** 343–391.

Crampin, S., 1984. Effective elastic-constants for wave propagation through cracked solids, in *Proc. First int. Workshop on Seismic Anisotropy,* Suzdal, 1982, eds Crampin, S., Hipkin, R. G. & Chesnokov, E. M., *Geophys. J. R. astr. Soc.*, **76,** 135–145.

Crampin, S., 1985a. Evaluation of anisotropy by shear-wave splitting, *Geophysics,* **50,** 142–152.

Crampin, S., 1985b. Evidence for aligned cracks in the Earth's crust, *First Break,* **3**(3), 12–15.

Crampin, S. & Atkinson, B. K., 1985. Microcracks in the Earth's crust, *First Break,* **3**(3), 16–20.

Crampin, S., Evans, R. & Atkinson, B. K., 1982. A new physical basis for prediction, *Eos,* **63,** 370.

Crampin, S., Evans, R. & Atkinson, B. K., 1984. Earthquake prediction: a new physical basis, in *Proc. First int. Workshop on Seismic Anisotropy,* Suzdal, 1982, eds Crampin, S., Hipkin, R. G. & Chesnokov, E. M., *Geophys. J. R. astr. Soc.*, **76,** 147–156.

Crampin, S., Evans, R. & Üçer, S. B., 1985. Analysis of records of local earthquakes: the Turkish Dilatancy Projects (TDP1 and TDP2), *Geophys. J. R. astr. Soc.*, **83,** 1–16.

Crampin, S., Evans, R., Üçer, B., Doyle, M., Davis, J. P., Yegorkina, G. V. & Miller, A., 1980. Observations of dilatancy-induced polarization anomalies and earthquake prediction, *Nature,* **286,** 874–877.

Crampin, S. & McGonigle, R., 1981. The variation of delays in stress-induced polarization anomalies, *Geophys. J. R. astr. Soc.*, **64,** 115–131.

Crampin, S., Stephen, R. A. & McGonigle, R., 1982. The polarization of *P*-waves in anisotropic media, *Geophys. J. R. astr. Soc.*, **68,** 477–485.

Doyle, M., 1981. The location of local earthquakes in a zone of anisotropy, *PhD dissertation,* University of Edinburgh.

Evans, R., 1984. Effects of the free surface on shear wavetrains, in *Proc. First int. Workshop on Seismic Anisotropy,* Suzdal, 1982, eds Crampin, S., Hipkin, R. G. & Chesnokov, E. M., *Geophys. J. R. astr. Soc.*, **76,** 165–172.

Evans, R., Asudeh, I., Crampin, S. & Üçer, S. B., 1985. Tectonics of the Marmara Sea region of Turkey: new evidence from microearthquake fault plane solutions, *Geophys. J. R. astr. Soc.*, **83**, 47–60.

Gal'perin, E. I., 1977. *The Polarization Method of Seismic Exploration* (in Russian), Nedra, Moscow; English translation, 1984, Reidel, Dordrecht.

Hadley, K., 1975. Azimuthal variation of dilatancy, *J. geophys. Res.*, **80**, 4845–4850.

Hubbert, M. K. & Willis, D. G., 1957. Mechanics of hydraulic fracture, *Trans. Am. Inst. Min. metall. Engrs*, **210**, 153–170.

Hudson, J. A., 1981. Wave speeds and attenuation of elastic waves in material containing cracks, *Geophys. J. R. astr. Soc.*, **64**, 133–150.

Hudson, J. A., 1982. Overall properties of a cracked solid, *Math. Proc. Camb. phil. Soc.*, **88**, 371–384.

Toksöz, M. N., Shakal, A. F. & Michael, A. J., 1979. Space-time migration of earthquakes along the North Anatolian Fault zone and seismic gaps. *Pure appl. Geophys.*, **117**, 1258–1270.

Weaver, C. S. & Hill, D. P., 1978. Earthquake swarms and local crustal spreading along major strike-slip faults in California, *Pure appl. Geophys.*, **117**, 51–64.

Zoback, M. L. & Zoback, M., 1980. State of stress in the conterminous United States, *J. geophys. Res.*, **85**, 6113–6156.

## Appendix: sources of observational error

The effects of anisotropy on seismic waves listed in Section 2 and modelled in Figs 2 and 3, are appropriate for propagation in an homogeneous anisotropic half-space. The crust of the Earth is not an homogeneous half-space, but it may be expected that the overall tectonic stress results in similar principal axes of stress throughout a large region despite the inhomogeneities and discontinuities within the region. This suggests that stress-induced cracks are likely to have similar orientations throughout the region even though the crack densities and crack dimensions may be different in different lithologies. Polarizations and delays behave differently in such circumstances. Polarizations are dependent principally on the symmetry of the anisotropy, whereas delays depend on the difference in the shear-wave velocities in the particular ray direction. Numerical experiments (Crampin 1978, 1981, 1985b) confirm that when the overall anisotropic symmetry of the media is preserved, the polarizations are a comparatively stable phenomenon. They show much more consistency than the delays for shear waves when propagating through different solids. It should also be noted that the observed polarization diagrams in this paper refer to waves propagating upwards from the earthquake source so that they are recorded within the shear-wave window. Thus most of the waves have almost normal incidence to any horizontal discontinuities and anomalies due to interactions at interfaces are small.

A considerable source of error is the lack of control in the determination of focal depths caused

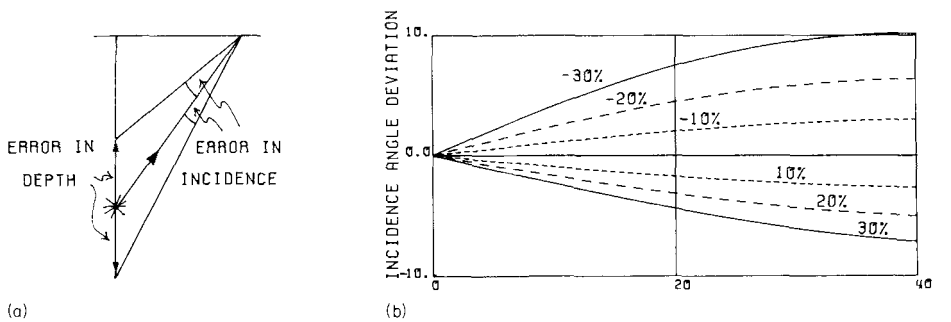


**Figure A1.** The effect of errors in depth on estimated angles of incidence. (a) Equal errors in depth above and below the real source result in larger and smaller errors, respectively, in the estimated angle of incidence. (b) Percentage deviation in incidence angle for errors in depth from −30 per cent (above the source) to +30 per cent (below the source) for angles of incidence from 0° to 40°.

by the trade-off between depth and origin time when local earthquakes are located only by direct arrivals from the upper focal sphere. The most significant effect of such errors in depth is that errors are introduced into the angles of incidence. Fig. A1 shows the effect of various percentages of errors in depth in increasing or decreasing the estimated incidence angle. These errors result in mislocations of arrivals in equal-area plots, so that the true positions of the polarizations and delays are scattered radially. Again, as with structural inhomogeneities, the largest effects are on the values of the delays between the split shear waves. The polarizations of the leading shear waves in the equal-area plots for vertical parallel cracks (Fig. 3) are approximately parallel to the strike of the cracks over almost the whole of the shear-wave window, and mislocations within the window will not significantly alter the overall pattern of the polarizations. In contrast, the delays between the split shear waves within the shear-wave window, vary over the whole range of values from zero to the maximum value so that small errors in location may severely disrupt the pattern of delays.

Recently, Cormier (1984) has shown that realistic irregular internal interfaces will rarely alter the polarization of shear waves by more than about 10°. It seems likely that topographic irregularities will cause similar deviations, so that the observed scatter of the polarizations of ±20° about N 100°E may well be caused by the structure and topography in this complicated area.